A review of possible optical absorption features of oxygen molecules in the icy surfaces of outer solar system bodies

Paul D. Cooper[a], Robert E. Johnson[b], Terence I. Quickenden[a],*

[a]*Chemistry, School of Biomedical and Chemical Sciences, The University of Western Australia, 35 Stirling Highway, Nedlands, WA 6009, Australia*
[b]*Engineering Physics, Thornton Hall B103, University of Virginia, Charlottesville, VA 22903-2442, USA*

Abstract

In this review we provide the data needed to interpret remote spectroscopic studies of O_2 molecules embedded in the icy surfaces of outer solar system bodies. O_2 produced by radiolysis has been seen in the gas phase and as the so-called 'solid O_2' trapped in the icy surfaces of Ganymede, Europa and Callisto. It may also have been indirectly observed on a number of objects by its radiolysis product, O_3. These observations indicate the importance of O_2 for understanding the chemical processes occurring on icy outer solar system surfaces. Therefore, the published absorption spectra of gaseous, liquid and solid O_2 and of O_2 embedded in H_2O ice are reviewed in some detail. Particular emphasis has been placed on the presentation of transition probabilities for the various O_2 spectral series so that their relative importances can be assessed when they are used for modelling the radiation chemistry occurring in such environments.
© 2003 Elsevier Science Ltd. All rights reserved.

1. Introduction

Water ice is often present on the surfaces of outer solar system bodies (Burns and Matthews, 1986) and there is increasing interest in the presence of oxygen molecules (O_2) either trapped in such icy surfaces (Johnson and Jesser, 1997; Johnson and Quickenden, 1997) or as an ambient gas (Johnson et al., 1998). It is well known (Reimann et al., 1984; Matich et al., 1993; Sieger et al., 1998; Westley et al., 1995) that O_2 is formed during photolytic and radiolytic laboratory experiments on ice and it is likely (Spencer et al., 1995; Calvin and Spencer, 1997) that similar O_2 formation occurs during the radiolysis of the icy surfaces in the outer solar system by plasma bombardment and during photolysis by solar UV.

The occurrence of radiolysis and photolysis on the surfaces of outer solar system icy moons is confirmed by the observation (Carlson et al., 1999) of the radiation product, hydrogen peroxide, in the UV and IR reflectance spectra of the surface of Europa. Recently, Moore and Hudson (2000)

showed that the formation of the peroxide at the surface temperatures of Ganymede and Europa may require O_2 or another oxidizer, such as CO_2, which is also known to be present (Carlson, 1999; McCord et al., 1997). The importance of oxygen in the outer solar system has been confirmed by the observations of excited O atoms which are thought to come from the dissociation of O_2 on Europa and Ganymede (Hall et al., 1995, 1998). It also is suggested by the observation of a 'solid form' of O_2 on the surface of Ganymede (Spencer et al., 1995; Calvin and Spencer, 1997). Recently, Spencer and Calvin (2002) have also reported a much weaker signal indicating solid O_2 is present on Europa and Callisto. Finally, a broad band in the UV, thought to be associated at least in part with O_3 in ice, has been tentatively identified in the reflectance spectrum of Ganymede (Noll et al., 1996) and the icy moons of Saturn (Noll et al., 1997). Since O_3 is not a direct product of the photolysis of ice (Gerakines et al., 1996), but is produced readily from condensed O_2, the observations suggest that O_2 may be ubiquitous in icy outer solar system bodies exposed to radiation.

In view of this growing interest in oxygen related signals from outer solar system bodies we feel it is important to review the data on oxygen absorption bands. Of particular interest is oxygen existing in its solid-state or as discrete

---

* Corresponding author. Fax: +61-8-9380-1005.
E-mail address: tiq@chem.uwa.edu.au (T.I. Quickenden).

oxygen molecules present in a host matrix. The environment provided by the host matrices may cause significant spectral shifts or intensity changes and these are given particular attention in this review. It is hoped that this review will assist in the planning of future spectroscopic measurements of the icy surface of outer solar system bodies as well as encourage a closer look at available remote sensing data and a re-examination of published fits to the observed data.

2. The absorption spectroscopy of O_2 in various environments

The UV, visible and near-infrared absorption features of the chromophores contained in icy surfaces of outer solar system bodies are useful for interpreting remote spectroscopic studies of such surfaces. Remote studies are usually done using reflectance spectroscopy where the observations show absorption through reduced reflectance at the absorption wavelength. We will now consider the optical absorption features of pure O_2 and of O_2 contained in ice.

A large number of absorption bands have been observed for the O_2 molecule in various conditions and states. Regrettably, there is a lack of information about the effect that adjacent H_2O molecules have on O_2 spectroscopy, with only a few cases reported in the literature. Many of the observations of O_2 absorption bands are from gas-phase measurements and while they will not give a true representation of the behaviour of O_2 embedded in water ice, they provide a reasonable starting point for such work. A summary of the gas-phase O_2 absorption bands is presented in Table 1. When there are high concentrations of O_2, such as found in liquid and solid O_2, absorption bands can be altered and additional bands can be induced (Landau et al., 1962). It has been suggested that the well-established O_2 present (Spencer et al., 1995; Calvin and Spencer, 1997) on the icy surface of Ganymede may exist as a solid. Hence the present review includes the spectroscopic characteristics of solid forms of O_2 and these are summarised in Table 2.

This review is primarily concerned with the optical absorption features of O_2 molecules. However there are also a number of emission bands that may also be detectable from icy surfaces. Matich et al. (1993) have observed the Herzberg emission of O_2 from UV-irradiated ices in laboratory studies and so it has been proposed by Johnson and Quickenden (1997) that emission from O_2, trapped within the icy surface of an outer solar system body, might be detectable from a probe in orbit above the surface. Remote sensing by reflectance spectroscopy has of course been used to examine outer solar system surfaces using ground based and orbiting telescopes such as the Hubble Space Telescope and the spectrometers on the Galileo probe. Although emission features may be important in future studies, the present paper is confined to the subject of absorptions features and

their possible effects on the reflectance spectra of outer solar system bodies.

While there have not been many extensive experimental studies which fully characterise O_2/H_2O matrices under the conditions found on outer solar system bodies, we have attempted in this review to present all the reported UV, visible and NIR electronic absorption bands of O_2 under a variety of conditions, but with an emphasis on situations where O_2 interacts with water lattices and/or other molecules that enhance O_2 absorptions. Many of these absorptions might generally be considered too weak to be measured from the surfaces of outer solar system bodies. However the assignment of two bands in the reflectance spectrum of Ganymede to weak O_2 absorption bands (Spencer et al., 1995; Calvin et al., 1996), suggests even such weak bands maybe important in telescopic studies. Alternatively, these bands may be enhanced by the H_2O matrix.

The electronic transitions of molecules can be dramatically altered by interaction with an ice lattice, as shown by the shift of the OH absorption at 309 nm in the gas phase to 280 nm in ice (Taub and Eiben, 1968). It is hoped that the present review will not only provide useful information for those studying O_2 on the surfaces of outer solar system bodies, but will also emphasise the need for more laboratory experiments on the spectroscopy of O_2 in ice matrices.

The detailed spectroscopic information in the sections that follow is summarised in Fig. 1. This provides a simplified overview showing the regions where the various O_2 spectral series exist and also indicates the peak oscillator strengths of each series in order to provide a quantity proportional to peak heights in optical absorption spectra.

2.1. The Herzberg absorption series

In 1932 Herzberg observed a series of absorption bands in molecular oxygen between the wavelengths of 240 and 270 nm (Herzberg, 1932). Herzberg assigned these absorptions to the symmetry forbidden transitions of the $A^3\Sigma_u^+ \leftarrow X^3\Sigma_g^-$ series. This system is designated as the Herzberg I series. The additional Herzberg II ($b^1\Sigma_u^- \leftarrow X^3\Sigma_g^-$) and Herzberg III ($A^3\Delta_u \leftarrow X^3\Sigma_g^-$) series were observed by Herzberg (1953) as weak lines amongst the much stronger Herzberg I lines. A detailed discussion of the identificatory history of these lines has been provided by Matich et al. (1993).

The transitions in all of the Herzberg series are electric dipole forbidden and are thus very weak. This is shown by the very small oscillator strengths in Table 1. However, the Herzberg electronic transitions are important with regards to the photochemistry of O_2. The *A–X*, *c–X* and *A′–X* absorption bands converge at 242 nm at which molecular O_2 dissociates to produce $O(^3P)$ atoms, which in turn can react with other O_2 molecules to produce ozone (O_3). While this is not the dominant photo-dissociation channel for producing O_3, it does contribute to its overall production.

Table 1
Spectroscopic absorption data for gas-phase O_2

Transition	Wavelength/nm (vibronic band in parentheses)	Oscillator strength	Integrated absorption cross-sections ($cm^2\ cm^{-1}$ molecule^{-1})	Method/state	Ref.
$a^1\Delta_g - X^3\Sigma_g^-$ Near-infrared Atmospheric oxygen	1269 (0,0) 1065 (1,0)	1.20×10^{-11} 1.70×10^{-12}	1.07×10^{-23} 1.50×10^{-24}	Fourier transform spectrometry/gas phase, 75% , O_2 : 25% N_2 200 K, 760 Torr	Smith and Newnham (2000)
$b^1\Sigma_g^+ - X^3\Sigma_g^-$ Atmospheric system	762.1 (0,0) 688.4 (1,0)	2.42×10^{-10} 1.70×10^{-11}	2.14×10^{-22} 1.50×10^{-23}	Fourier transform spectrometry/gas phase, 21% O_2 : 79% N_2, 300 K, 760 Torr	Newnham and Ballard (1998)
$c^1\Sigma_u^- - X^3\Sigma_g^-$ Herzberg II system	292.6 (2,0) 286.6 (3,0) 281.2 (4,0) 276.1 (5,0) 271.2 (6,0) 267.3 (7,0) 263.5 (8,0) 260.0 (9,0) 256.9 (10,0) 254.1 (11,0) 251.6 (12,0) 249.4 (13,0) 247.6 (14,0) 246.0 (15,0) 244.7 (16,0) 243.8 (17,0) 243.1 (18,0) 242.7 (19,0)	6.78×10^{-14} 2.26×10^{-13} 5.31×10^{-13} 9.94×10^{-13} 1.67×10^{-12} 2.52×10^{-12} 3.50×10^{-12} 4.52×10^{-12} 5.31×10^{-12} 6.33×10^{-12} 7.35×10^{-12} 6.44×10^{-12} 6.78×10^{-12} 6.67×10^{-12} 5.09×10^{-12} 4.07×10^{-12} 2.26×10^{-12} 9.49×10^{-13}	6.00×10^{-26} 2.00×10^{-25} 4.70×10^{-25} 8.80×10^{-25} 1.48×10^{-24} 2.23×10^{-24} 3.10×10^{-24} 4.00×10^{-24} 4.70×10^{-24} 5.60×10^{-24} 6.50×10^{-24} 5.70×10^{-24} 6.00×10^{-24} 5.90×10^{-24} 4.50×10^{-24} 3.60×10^{-24} 2.00×10^{-25} 8.40×10^{-25}	Fourier transform spectrometry/gas phase, 100% O_2, 293 K, 20–750 Torr[a]	Mèrienne et al. (2000)
$A'^3\Delta_u - X^3\Sigma_g^-$ Herzberg III system[b]	277.1 (2,0)[c] 278.2 (2,0)[d] 271.6 (3,0)[c] 272.7 (3,0)[d] 266.6 (4,0)[c] 267.7 (4,0)[d] 262.0 (5,0)[c] 263.0 (5,0)[d] 257.9 (6,0)[c] 258.9 (6,0)[d] 254.2 (7,0)[c] 255.1 (7,0)[d] 250.9 (8,0)[c] 251.8 (8,0)[d] 248.1 (9,0)[c] 248,9 (9,0)[d] 245.7 (10,0)[c] 246.5 (10,0)[d] 243.9 (11,0)[c] 244.6 (11,0)[d] 242.7 (12,0)[c] 243.3 (12,0)[d]	3.84×10^{-13} 1.15×10^{-12} 2.68×10^{-12} 5.24×10^{-12} 8.72×10^{-12} 1.22×10^{-11} 1.58×10^{-11} 1.73×10^{-11} 1.79×10^{-11} 1.35×10^{-11} 6.97×10^{-12}	3.40×10^{-25} 1.02×10^{-24} 2.37×10^{-24} 4.64×10^{-24} 7.72×10^{-24} 1.08×10^{-23} 1.40×10^{-23} 1.53×10^{-23} 1.58×10^{-23} 1.19×10^{-23} 6.17×10^{-24}	Fourier transform spectrometry/gas phase, 100% O_2, 293 K, 20–750 Torr[a]	Mèrienne et al. (2000)
$A^3\Sigma_u^+ - X^3\Sigma_g^-$ Herzberg I system	285.6 (0,0) 279.5 (1,0) 273.8 (2,0) 268.6 (3,0) 263.8 (4,0) 259.4 (5,0) 255.5 (6,0) 252.0 (7,0) 248.9 (8,0) 246.4 (9,0) 244.4 (10,0) 243.0 (11,0)	8.36×10^{-14} 8.02×10^{-13} 3.73×10^{-12} 1.11×10^{-11} 2.51×10^{-11} 5.09×10^{-11} 8.36×10^{-11} 1.22×10^{-10} 1.57×10^{-10} 1.79×10^{-10} 1.64×10^{-10} 9.15×10^{-11}	7.40×10^{-26} 7.10×10^{-25} 3.30×10^{-24} 9.82×10^{-24} 2.22×10^{-23} 4.50×10^{-23} 7.40×10^{-23} 1.08×10^{-22} 1.39×10^{-22} 1.58×10^{-22} 1.45×10^{-22} 8.10×10^{-23}	Fourier transform spectrometry/gas phase, 100% O_2, 293 K, 20–750 Torr[a]	Mèrienne et al. (2000)
$B^3\Sigma_u^- - X^3\Sigma_g^-$ Schumann–Runge system	202.6 (0,0) 199.8 (1,0) 197.2 (2,0)	3.45×10^{-10} 3.90×10^{-9} 2.38×10^{-8}	3.05×10^{-22} 3.45×10^{-21} 2.10×10^{-20}	Conventional spectroscopy/gas phase, 100% O_2,	Ackerman et al. (1970) and Fugol et al. (1976)

Table 1 (*continued*)

Transition	Wavelength/nm (vibronic band in parentheses)	Oscillator strength	Integrated absorption cross-sections (cm^2 cm^{-1} $molecule^{-1}$)	Method/state	Ref.
	194.8 (3,0)	9.90×10^{-8}	8.75×10^{-20}	300 K, various pressures	
	192.4 (4,0)	3.21×10^{-7}	2.84×10^{-19}		
	190.3 (5,0)	8.52×10^{-7}	7.53×10^{-19}		
	188.2 (6,0)	1.91×10^{-6}	1.69×10^{-18}		
	186.4 (7,0)	3.81×10^{-6}	3.37×10^{-18}		
	184.7 (8,0)	6.68×10^{-6}	5.91×10^{-18}		
	183.1 (9,0)	1.06×10^{-5}	9.39×10^{-18}		
	181.6 (10,0)	1.57×10^{-5}	1.39×10^{-17}		
	180.4 (11,0)	2.09×10^{-5}	1.85×10^{-17}		
	179.3 (12,0)	2.53×10^{-5}	2.24×10^{-17}		
	178.3 (13,0)	2.88×10^{-5}	2.55×10^{-17}		
	177.5 (14,0)	3.03×10^{-5}	2.68×10^{-17}		
	176.8 (15,0)	2.92×10^{-5}	2.58×10^{-17}		
	176.3 (16,0)	2.59×10^{-5}	2.29×10^{-17}		
	175.9 (17,0)	2.23×10^{-5}	1.97×10^{-17}		
	175.6 (18,0)	1.83×10^{-5}	1.62×10^{-17}		
	175.3 (19,0)	1.44×10^{-5}	1.27×10^{-17}		

[a]The Herzberg I bands were measured predominantly at low pressures to prevent possible interference from Herzberg II and III lines. Herzberg II and III bands can only be measured at higher pressures because they are much weaker transitions than the Herzberg I transitions.

[b]Although the $A'^3\Delta_u$ state should produce 3 sub-bands due to spin–orbit coupling, it was found that the $\Omega = 3$ sub-band only accounted for ca. 10% of the integrated absorption cross-section for each vibrational level and has thus been omitted from this table. The relevant data was also incomplete due to the difficulty of detecting such a weak series of lines. Oscillator strength and integrated absorption cross-sections are calculated as the sum of the $\Omega = 1, 2, 3$ bands.

[c]$\Omega = 1$ band.

[d]$\Omega = 2$ band.

Ozone has recently been tentatively assigned to a band observed in the reflectance spectra of a number of icy satellite surfaces (Noll et al., 1996, 1997). If stable quantities of oxygen on outer solar system bodies are exposed to high-energy radiation, then this pathway will produce O_3.

$$O_2 + h\nu \rightarrow O + O, \tag{1}$$

$$O + O_2 \rightarrow O_3. \tag{2}$$

Although many of the O_2 bands are weak, O_3 absorption bands in the UV are relatively strong. Ozone is not a primary radiation product of water ice and cannot be produced without the presence of O_2, thus O_3 may act as a "tracer" molecule to diagnose the presence of O_2 molecules on outer solar system bodies. It is evident that an understanding of this process and a determination of the extent to which O_2 dissociation in the Herzberg continuum occurs on outer solar system bodies, is of importance.

Gas phase experiments (Mèrienne et al., 2000) have shown that the $A–X$ bands in the Herzberg series are ca. an order of magnitude larger than the $c–X$ and $A'–X$ transitions. However, this trend is not seen in perturbed O_2 systems where a single O_2 molecule's electronic orbitals are slightly altered by the interaction of a nearby molecule, as is especially the case where the O_2 is embedded in a host matrix. The breakdown of optical selection rules by a

solid-state matrix results in the enhancement of the $A'–X$ transitions (Goodman and Brus, 1977; Slanger and Cosby, 1988). The normally dominant gas phase $A–X$ bands are observed to be very weak in comparison with the $A'–X$ bands in studies of O_2 in nitrogen, argon and xenon matrices (Goodman and Brus, 1977).

A further example of a dramatic perturbation of weak absorptions is provided by the weakly bound $(O_2)_2$ gas-phase moiety. Shardanand (1969) has reported that the absorption cross-section of the $A'^3\Delta_u + X^3\Sigma_g^- \leftarrow X^3\Sigma_g^- + X^3\Sigma_g^-$ transition of weakly bound $(O_2)_2$ in the gas phase is 10^3 times greater than the corresponding $A'^3\Delta_u \leftarrow X^3\Sigma_g^-$ transition of isolated O_2. Thus, it would appear that even a small interaction from a weakly bound molecule (in this present case another O_2 molecule or in the solid-state matrix case from $(N_2)_x$, Ar_x or Xe_x) can significantly perturb an O_2 molecule, and cause some previously highly forbidden transitions to become more probable. These absorptions occur in the same region as the ozone-like features observed from Ganymede. However, due to the weak nature of these transitions, it is unlikely that they contribute significantly to the observed absorption band unless they are perturbed in such a way as to further enhance their transition probabilities or unless O_2 was present in sufficient quantities to overcome its weak absorption. There is little experimental research on the

Table 2
Spectroscopic absorption data for gas-phase O_2

Transition	Wavelength/nm (vibronic band in parentheses)	Oscillator strength	Integrated absorption cross-sections (cm^2 cm^{-1} $molecule^{-1}$)	Method/state	Ref.
$a^1\Delta_g - X^3\Sigma_g^-$	1252 (0,0)	2.0×10^{-7}	1.8×10^{-19}	α-O_2 20.6 K	Landau et al. (1962)
	1056 (1,0)	6.6×10^{-8}	5.9×10^{-20}		
	914.9 (2,0)	9.7×10^{-9}	8.6×10^{-21}		
	808.9 (3,0)	1.8×10^{-9}	1.6×10^{-21}		
$b^1\Sigma_g^+ - X^3\Sigma_g^-$	756.4 (0,0)	9.7×10^{-9}	8.6×10^{-21}	α-O_2 20.6 K	Landau et al. (1962)
$a^1\Delta_g + a^1\Delta_g - X^3\Sigma_g^- + X^3\Sigma_g^-$	627.1 (0,0)	3.9×10^{-7}	3.4×10^{-19}	α-O_2 20.6 K	Landau et al. (1962)
	576.3 (1,0)	4.3×10^{-7}	3.8×10^{-19}		
	531.7 (2,0)	3.1×10^{-8}	2.8×10^{-20}		
	494.2 (3,0)	6.2×10^{-9}	5.5×10^{-21}		
$a^1\Delta_g + a^1\Delta_g - X^3\Sigma_g^- + X^3\Sigma_g^-$	628.1 (0,0)	1.1×10^{-7}	9.6×10^{-20}	β-$O_2 \sim 35$ K	Landau et al. (1962)
	577.4 (1,0)	1.2×10^{-7}	1.0×10^{-19}		
	532.5 (2,0)	2.3×10^{-8}	2.0×10^{-20}		
	494.6 (3,0)	2.9×10^{-9}	2.5×10^{-21}		
$a^1\Delta_g + a^1\Delta_g - X^3\Sigma_g^- + X^3\Sigma_g^-$	629.7 (0,0)	2.5×10^{-8}	2.2×10^{-20}	γ-$O_2 \sim 49$ K	Landau et al. (1962)
	577.7 (1,0)	4.8×10^{-8}	4.3×10^{-20}		
	532.8 (2,0)	2.7×10^{-9}	2.4×10^{-21}		
$a^1\Delta_g + b^1\Sigma_g^+ - X^3\Sigma_g^- + X^3\Sigma_g^-$	474.8 (0,0)	2.8×10^{-8}	2.5×10^{-20}	α-O_2 20.6 K	Landau et al. (1962)
	446.0 (1,0)	1.6×10^{-8}	1.4×10^{-20}		
	419.9 (2,0)	9.0×10^{-9}	7.9×10^{-21}		
	397.2 (3,0)	9.7×10^{-10}	8.6×10^{-22}		
$a^1\Delta_g + b^1\Sigma_g^+ - X^3\Sigma_g^- + X^3\Sigma_g^-$	476.2 (0,0)	8.4×10^{-9}	7.4×10^{-21}	β-$O_2 \sim 35$ K	Landau et al. (1962)
	447.1 (1,0)	6.8×10^{-9}	6.0×10^{-21}		
$a^1\Delta_g + b^1\Sigma_g^+ - X^3\Sigma_g^- + X^3\Sigma_g^-$	477.0 (0,0)	3.3×10^{-9}	2.9×10^{-21}	γ-$O_2 \sim 49$ K	Landau et al. (1962)
$b^1\Sigma_g^+ + b^1\Sigma_g^+ - X^3\Sigma_g^- + X^3\Sigma_g^-$	378.4 (0,0)	1.7×10^{-8}	1.5×10^{-20}	α-O_2 20.6 K	Landau et al. (1962)
	360.8 (1,0)	4.7×10^{-8}	4.1×10^{-20}		
	343.7 (2,0)	3.1×10^{-8}	2.8×10^{-20}		

absorption bands of solid oxygen or oxygen/water matrices in this UV region to predict if any such enhancements are likely to contribute to the recent Ganymede observations.

The effects of a weakly bound H_2O molecule on the Herzberg series of solid state O_2 are unknown. However, absorption spectra of O_2-saturated liquid water show greater absorption cross-sections than pure liquid water at wavelengths below ca. 250 nm (Heidt and Ekstrom, 1957). Two processes may contribute to this enhancement.

Firstly, a contribution is proposed from the absorption of a weakly bound $H_2O \cdot O_2$ complex. Recent theoretical studies of this complex (Byers Brown et al., 1992; Byers Brown, 1995) have shown that it may absorb a photon in the 200–250 nm region of the UV spectrum (the region of the Herzberg continuum) via the formation of the charge transfer complex $H_2O^+ \cdot O_2^-$. This also overlaps the region identified as the ozone-like feature on Ganymede. Calculations have also shown that although $H_2O \cdot O_2$ is weakly bound, with a calculated binding energy of 3.0 kJ mol^{-1}

(Kjaergaard et al., 2002), it may be a significant complex in the gas phase (Svishchev and Boyd, 1998; Vaida and Headrick, 2000). However, no literature has appeared on the existence of such complexes in H_2O/O_2 ices. Irradiated ices containing oxygen and water may well contain stable $H_2O \cdot O_2$ complexes that could potentially be significant in the chemistry and spectroscopy of such ices.

A second reason may be a relaxation of the selection rules for the Herzberg bands by complexation of O_2 with a partner molecule. The Herzberg bands are forbidden transitions but the selection rules are indeed relaxed by the formation of say $(O_2)_2$ or $H_2O \cdot O_2$, as previously described. There is some evidence (Palmer et al., 1996) to suggest that both the charge-transfer absorption and the activated forbidden Herzberg continuum absorption may occur simultaneously in chemical processes in the Earth's atmosphere.

Like the broad continuum assigned to the H_2O_2 observed at Europa (Carlson et al., 1999), the absorption of oxygen-saturated liquid water, which is tentatively at-
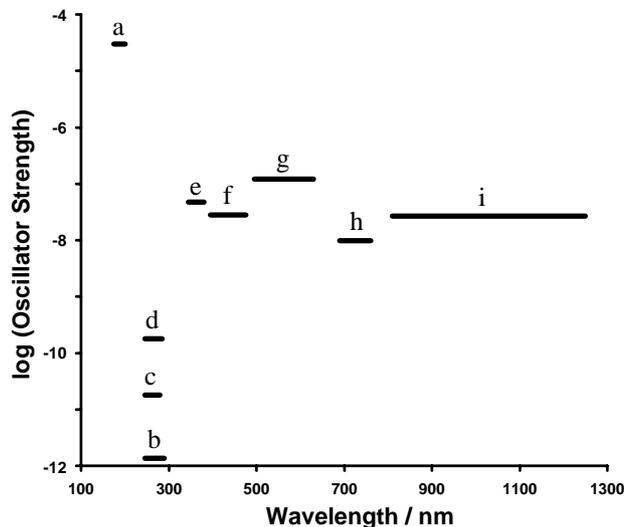
Fig. 1. The maximum oscillator strength for each O_2 absorption series. This diagram indicates the approximate wavelength range of each absorption band but it should be noted that the oscillator strength shown for each absorption series is only the maximum value for that series and is not necessarily a representative value for all wavelengths in the band. Tables 1 and 2 should be consulted for more detailed data. (a) Gas-phase Schumann–Runge series; Fugol et al. (1976). (b) Gas-phase Herzberg II series; Mèrienne et al. (2000). (c) Gas-phase Herzberg III series; Mèrienne et al. (2000); (d) Gas-phase Herzberg I series; Mèrienne et al. (2000). (e) α-O_2 $b^1\Sigma_g^+ + b^1\Sigma_g^+ - X^3\Sigma_g^- + X^3\Sigma_g^-$ series; Landau et al. (1962). (f) β-O_2 $a^1\Delta_g + b^1\Sigma_g^+ - X^3\Sigma_g^- + X^3\Sigma_g^-$ series; Landau et al. (1962). (g) β-O_2 $a^1\Delta_g + a^1\Delta_g - X^3\Sigma_g^- + X^3\Sigma_g^-$ series; Landau et al. (1962). (h) α-O_2 Atmospheric series; Landau et al. (1962). (i) α-O_2 NIR Atmospheric series; Landau et al. (1962).

tributed to the absorption of an $H_2O \cdot O_2$ complex (Byers Brown, 1995), has a similar trend to increasing absorption in the far-UV. However the absorption in this region by O_2-saturated liquid water is many orders of magnitude less than that of H_2O_2 (Heidt and Ekstrom, 1957; Molina et al., 1977) and therefore may not contribute significantly to the observed absorption feature.

In H_2O/O_2 ices, such as those proposed to exist on the surfaces of some outer solar system bodies, the above Herzberg series absorptions by O_2 may be important, not only in the better identification and characterisation of such ices, but also in the understanding of their photochemistry. It is clearly of particular importance to carry out more laboratory based research on the existence of $H_2O \cdot O_2$ complexes in oxygenated and/or irradiated ices.

2.2. The visible atmospheric system of O_2

This series, which dates back to the work of Wollaston in 1802 and Fraunhofer in 1817, was first assigned by Mulliken (1928) to the $b^1\Sigma_g^+ \leftarrow X^3\Sigma_g^-$ transitions via the bands observed in laboratory absorption and atmospheric absorption measurements. Newnham and Ballard (1998) have recently applied Fourier transform spectrometry to probe the 762.1 nm (0,0) and 688.4 nm (1,0) b–X transitions. Table 1

summarises this data. Unlike many of the other electronic transitions of O_2 in which high densities enhance the absorption cross-sections, there is no such enhancement of the $b^1\Sigma_g^+ \leftarrow X^3\Sigma_g^-$ bands (Dianov-Klokov, 1966). In fact the integrated absorption cross-section of solid O_2 is smaller than that of gas-phase O_2 as shown in Table 2, making the $b^1\Sigma_g^+ \leftarrow X^3\Sigma_g^-$ transition one of the weaker solid O_2 absorption series. For this reason, it is unlikely to be of much significance in the spectroscopy of outer solar system bodies.

2.3. The near-infrared electronic transitions of O_2

The $a^1\Delta_g \leftarrow X^3\Sigma_g^-$ series of O_2 was first predicted by Mulliken (1928) and was first observed by Ellis and Kneser (1933) in the absorption spectrum of liquid oxygen. Recent work by Smith and Newnham (2000) using Fourier transform spectrometry has provided highly resolved spectra of the $a^1\Delta_g \leftarrow X^3\Sigma_g^-$ (0,0) and (1,0) bands, resulting in the accurate determination of absolute gas-phase absorption cross-sections.

The gas-phase $a^1\Delta_g \leftarrow X^3\Sigma_g^-$ O_2 spectra consist of rotational fine structure with an underlying absorption continuum. Smith and Newnham (1999) have shown that these continua can be deconvoluted into two components, one component having a linear dependence on the partial pressure of O_2 ($p(O_2)$) and the remaining component having a quadratic dependence. This suggests that the $p(O_2)$-dependent absorption components are related to the absorptions by a single O_2 molecule, while the $p(O_2)^2$-dependent absorption components are absorptions by an $(O_2)_2$ complex. Smith and Newnham (2000) experimented with diluting the O_2 with N_2 and observed an increase in the square dependent component with increasing N_2 concentration, probably due to absorption by an O_2–N_2 transient complexes. This may be due to the breakdown of the selection rules for O_2 in the presence of N_2.

With increasing density, and thus with greater perturbation from gas-phase conditions, the $a^1\Delta_g \leftarrow X^3\Sigma_g^-$ absorption bands, like many of the O_2 absorptions, become more intense (Dianov-Klokov, 1966). As shown in Tables 1 and 2, the (0–0) and (1–0) bands in the solid-state show an increase in intensity of ca. 4 orders of magnitude compared with those observed in the gas-phase. The integrated absorption coefficient of the (0–0) $a^1\Delta_g \leftarrow X^3\Sigma_g^-$ band is comparable with the $a^1\Delta_g + a^1\Delta_g \leftarrow X^3\Sigma_g^- + X^3\Sigma_g^-$ O_2 absorptions that have been assigned to the 627.5 and 577.2 nm features on Ganymede. The (0–0) and (1–0) $a^1\Delta_g \leftarrow X^3\Sigma_g^-$ bands of O_2 may contribute to the absorption in the regions of ~ 1050 and ~ 1250 nm that are observed on a number of the icy satellites. This is a region where water has two weak absorption bands (Calvin et al., 1996). However, the effects of grain size, hydrated minerals (McCord et al., 1999a, b) and temperature (Grundy et al., 1999) complicate the interpretations of these absorption bands. The possible contribution of O_2 absorption has not been thoroughly explored

although Calvin et al. (1996) proposed that O_2 absorption in this region might be significant.

Grundy et al. (1999) have reported reflectance spectra for a number of Jovian, Saturnian and Uranian satellites. All of these spectra show relatively strong absorptions at 1.5 and 2.0 μm that are characteristic of water. However, we note that the spectra of Europa and Ganymede show considerably greater band depths for the 1.25 μm band than those of all the other icy satellites examined. Due to the large number of variables that affect absorption bands in this region, it is difficult to know the reason for these differences. However, the possibility that the differences in the 1.25 μm region of the spectra are due to O_2 absorption must be considered, along with the possibility they are due to grain size, the presence of hydrated minerals and temperature differences.

2.4. The Schumann–Runge absorption bands of O_2

The Schumann–Runge bands of oxygen are the most extensively studied bands of molecular oxygen, and arise from the most intense transitions. These bands occur in the UV region between 175 and 200 nm as 20 absorption features representing transitions from the $X^3\Sigma_g^-$ ground vibrational state to the excited $B^3\Sigma_u^-$ state, as shown in Table 1. Electronic transitions to the $B^3\Sigma_u^-$ excited state from vibrationally excited $X^3\Sigma_g^-$ states of O_2 have also been observed but only at high temperatures (Hudson and Carter, 1968) and thus can be disregarded in the present discussion.

The Schumann–Runge system plays an important part in O_2 photochemistry. Not only does the Schumann–Runge absorption continuum result in photodissociation of O_2 in the 135–175 nm region to $O(^1D)$ and $O(^3P)$ atoms, but the $B^3\Sigma_u^-$ state is intersected by the repulsive $^3\Pi_u$ state. This provides an additional source of $O(^3P)$ atoms via predissociation from a majority of the $B^3\Sigma_u^-$ upper states (Krupenie, 1972). Therefore atomic oxygen produced by photolysis must be accounted for not only by absorption in the Herzberg $(O(^3P) + O(^3P))$ and Schumann–Runge $(O(^3P) + O(^1D))$ continua, but also by predissociation from the Schumann–Runge absorption bands that provide an extra source of $O(^3P)$ atoms from absorption in the 175–195 nm region.

The spectrum of the Schumann–Runge region of solid oxygen (Romand and Granier-Mayence, 1954) shows an absorption continuum in the 150–200 nm region. No vibronic bands were observed in that work. These workers suggested that the absorption bands may have been too weak to be observed with the sample thickness used and the resolution of their equipment may have not been adequate. Observations using thicker samples were not possible due to diffusion of the incident radiation.

2.5. Condensed O_2 dimer absorption bands

These absorption features are currently attracting considerable attention. The so-called O_2 dimer absorptions

$a^1\Delta_g + a^1\Delta_g \leftarrow X^3\Sigma_g^- + X^3\Sigma_g^-$ at 627 and 577 nm have been assigned to spectral features observed from the surface of Ganymede (Spencer et al., 1995; Calvin and Spencer, 1997), Europa and Callisto (Spencer and Calvin, 2002). High-pressure gas phase, liquid and solid phase O_2 is interesting because at these high densities, double electronic transitions can occur between a pair of interacting O_2 molecules. When this occurs, the wavelength of the absorption of an interacting O_2 pair is approximately halved compared with the corresponding single electronic transition of an isolated O_2 molecule. Thus, the energy of one photon appears to be split between two electronic excitations of two interacting O_2 molecules.

The phrase "a pair of interacting O_2 molecules" has been used here rather than the phrase "an $(O_2)_2$ oxygen dimer" because of the implication from the latter that high density forms of O_2 exist exclusively as stable discrete dimers. Low temperature, gas-phase studies (Long and Ewing, 1971) have provided some evidence for the formation of stable $(O_2)_2$, but clearly the interaction is not sufficient to induce any significant structural changes in the solid phase, as the analyses of α, β and γ phases of solid O_2 (Jordan et al., 1964; Cairns and Pimentel, 1965) show no evidence for any discrete dimer molecules.

If the intensities of the dimer absorption bands were proportional to the number of dimers present in a sample, then one would expect greater band intensities at lower temperatures where the dimers would be more stable. Dianov-Klokov (1966) however has shown that at a constant density (1.17 g cm^{-3}) the dimer absorption bands increase in intensity by a factor of between 1.41 and 3.14 times over the temperature range 80–250 K. This supports the notion that under these conditions, a collision pair of O_2 molecules is predominantly the main absorbing species. A similar trend is observed for the three solid phases of O_2, but this kinetic model is not applicable to the rigid structures in O_2 crystal lattices. The densities of α-, β- and γ-O_2 (Roder, 1978) are similar enough to not account for the differences in absorption cross-section, so it is likely that the differences in the crystal structure for the phases of solid O_2 affect the degree of activation of these forbidden transitions.

Each phase has a particular band shape. The analysis of the 577 and 627 nm bands observed from Ganymede by Spencer et al. (1995) showed that the features were most like that of β-O_2. While it is clear that β-O_2 cannot exist at the temperatures on the surface of Ganymede (Orton et al., 1996), if other bands in this dimer series could be detected it might be possible to determine the state in which O_2 is present within Ganymede's surface.

A recent measurement of the reflectance spectra from O_2 co-deposited on a cold substrate with H_2O shows slight shifts in the $(O_2)_2$ band positions and changes in the band shapes (Vidal et al., 1997; Baragiola and Bahr, 1999). These have been used to suggest that the observed oxygen is not trapped in ice, but this position has been questioned (Johnson, 1999).

Very recent work (Calvin et al., 2002) has shown that the band strengths of the absorptions of liquid O_2 are strongly dependent on temperature and density. While previous work (Landau et al., 1962; Vidal et al., 1997; Baragiola and Bahr, 1999) does not provide a precise spectral match in terms of band position, depth and shape, the systematic approach of making laboratory measurements on O_2 under various conditions (e.g. at different temperatures and densities, as a solid or liquid, and with impurities such as H_2O and/or O_3) provides the best approach for understanding the high-density O_2 spectral features of Ganymede, Europa and Callisto.

3. Summary

Because a number of the icy satellites of the giant planets are embedded in an intense radiation field, the radiation products of ice should be seen in or near the surface ice of such satellites. Indeed, a number have been seen. One such product is molecular oxygen, the focus of this paper. Based on the ratio of the transitions among the ground state multiplets of atomic O, O_2 has been suggested to be present in the gas phase at Europa and Ganymede (Hall et al., 1995), as predicted due to radiolysis of ice (Johnson et al., 1982). In addition, $O(^1D)$ has been seen in the equatorial regions of Ganymede (Brown and Boucher, 1999). However, gas-phase molecular oxygen has not been identified directly because of its low column abundances and its weak absorbance at those wavelengths where the solar radiation is most intense as seen in Table 1. A column abundance of the order of a few times 10^{15} O_2/cm^2 has been estimated for the gas phase over the surface of Europa, the net absorbance in the Schumann–Runge system would be of the order of 1% at the shortest wavelengths.

Based on laboratory measurements of the matrix perturbations on the absorption cross-section, O_2 is more easily observed as O_2 in the surface ice. However, although these bands have much larger absorbances, they still require considerable column abundances to be seen in reflectance in the near UV, visible and NIR. In spite of this, a 'solid' form of O_2 has apparently been seen at Ganymede, Europa and Callisto. Based on the band positions, the form of O_2 appears to most closely resemble β-O_2. This is surprising because the expected temperature differs significantly from that for β-O_2 and indeed at the nominal surface temperatures solid O_2 is not stable. However, the band shapes differ from that of β-O_2, therefore, the observed O_2 is likely to be either trapped in ice or adsorbed on grains in the regolith. Additional laboratory studies are required on the production of these bands in a number of likely environments.

In the short term, indirect detection of gas-phase O_2 may remain the best possibility for further studies of the production of O_2 by radiolysis and photolysis. McGrath et al. (2000) have observed the intensities of the ground state mul-

tiplet of O across the surface of Europa and have noted correlations to spatial variations in the surface geology. Such can be used to look for the O_2 source regions. Alternatively, since the formation of O_3 indicates the presence of O_2, O_3 can be used as a tracer molecule via the observation of the strong Hartley band absorption (Noll et al., 1996). For instance, using the rate equations (Johnson and Quickenden, 1997; as corrected in Johnson, 1999) a ratio $O_3/O_2 \sim 0.01$ is expected due to photolysis alone. Although such studies are less satisfactory than direct detection of O_2, they provide strong motivation for further observation and laboratory studies. This is particularly so since the ozone-like band differs from pure O_3, possibly due to the presence of other impurities (Johnson, 2001) or to perturbations like those described here.

References

Ackerman, M., Biaumé, F., Kockarts, G., 1970. Absorption cross sections of the Schumann–Runge bands of molecular oxygen. Planet. Space Sci. 18, 1639–1651.

Baragiola, R.A., Bahr, D.A., 1999. Laboratory studies of the optical properties and stability of oxygen on Ganymede. J. Geophys. Res. 104, 14179–14182.

Brown, M.E., Boucher, A.H., 1999. Observations of Ganymede's visible aurora. Bull. Amer. Astron. Soc. 31, 1183.

Burns, J.A., Matthews, M.S. (Eds.), 1986. Satellites. University of Arizona Press, Tucson.

Byers Brown, W., 1995. Photonucleation of water vapour in the presence of oxygen. Chem. Phys. Lett. 235, 94–98.

Byers Brown, W., Vincent, M.A., Trollope, K., Hillier, I.H., 1992. Van der Waals and charge complex-transfer complexes of molecular oxygen and water. Chem. Phys. Lett. 192, 213–216.

Cairns, B.R., Pimentel, G.C., 1965. Infrared spectra of solid α- and β-oxygen. J. Chem. Phys. 43, 3432–3438.

Calvin, W.M., Spencer, J.R., 1997. Latitudinal distribution of O_2 on Ganymede: observations with the Hubble Space Telescope. Icarus 120, 505–516.

Calvin, W.M., Johnson, R.E., Spencer, J.R., 1996. O_2 on Ganymede: spectral characteristics and plasma formation mechanisms. Geophys. Res. Lett. 23, 673–676.

Calvin, W.M., Anicich, V.G., Brown, R.H., 2002. Visible and near-infrared transmission spectra of condensed oxygen: temperature and phase effects. Icarus, submitted for publication.

Carlson, R.W., 1999. A tenuous carbon dioxide atmosphere on Jupiter's moon Callisto. Science 283, 820–821.

Carlson, R.W., Anderson, M.S., Johnson, R.E., Smythe, W.D., Hendrix, A.R., Barth, C.A., Soderblom, L.A., Hansen, G.B., McCord, T.B., Dalton, J.B., Clark, R.N., Shirley, J.H., Ocampo, A.C., Matson, D.L., 1999. Hydrogen peroxide on the surface of Europa. Science 283, 2062–2064.

Dianov-Klokov, V.I., 1966. Absorption of condensed oxygen in the 1.26–0.3 µ region. Opt. Spektrosk. 20, 954–962.

Ellis, J.W., Kneser, H.O., 1933. Combination relations in the absorption of liquid oxygen. Z. Phys. 86, 583–591.

Fugol, I.Ya., Gimpelevich, L.G., Timchenko, L.I., 1976. Electronic-vibrational states of oxygen in inert-gas crystals for the Schumann–Runge system. Opt. Spectrosc. 40, 159–163.

Gerakines, P.A., Shutte, W.A., Ehrenfreund, P., 1996. Ultraviolet processing of interstellar ice analogs. Astron. Astrophys. 312, 289–305.

Goodman, J., Brus, L.E., 1977. Electronic spectroscopy and dynamics of the low-lying $A^3\Sigma_u^+$, $C^3\Delta_u$ and $c^1\Sigma_u^-$ states of O_2 van der Waals solids. J. Chem. Phys. 67, 1482–1490.

Hall, D.T., Strobel, D.F., Feldman, P.D., McGrath, M.A., Weaver, H.A., 1995. Detection of an atmosphere on Jupiter's moon Europa. Nature 373, 677–679.

Hall, D.T., Feldman, P.D., McGrath, M.A., Strobel, D.F., 1998. The far-ultraviolet oxygen airglow of Europa and Ganymede. Astrophys. J. 499, 475–481.

Heidt, L.J., Ekstrom, L., 1957. Influence of dissolved air on optical density measurements of water solutions. J. Am. Chem. Soc. 79, 1260–1261.

Herzberg, G., 1932. A new "forbidden" absorption band system of the O_2 molecule. Naturwissenschatten 20, 577.

Herzberg, G., 1953. Forbidden transitions in diatomic molecules. III. New $^1\Sigma_u^- \leftarrow X^3\Sigma_g^-$ and $^3\Delta_u \leftarrow X^3\Sigma_g^-$ absorption bands of the oxygen molecule. Can. J. Phys. 31, 657–669.

Hudson, R.D., Carter, V.L., 1968. Absorption at elevated temperature (300 to 900 K) in the Schumann–Runge system. J. Opt. Soc. Am. 58, 1621–1629.

Johnson, R.E., 1999. Comment on "Laboratory studies of the optical properties and stability of oxygen on Ganymede". J. Geophys. Res. 104, 14179–14182.

Johnson, R.E., 2001. Surface Chemistry in the Jovian Magnetosphere Radiation Environment. In: Dessler, R. (Ed.), Chemical Dynamics in Extreme Environments, Adv. Ser. Phys. Chem. Vol .11, pp. 390–419. World Scientific, Singapore (Chap. 8).

Johnson, R.E., Jesser, W.A., 1997. O_2/O_3 microatmospheres in the surface of Ganymede. Astrophys. J. 480, L79–L82.

Johnson, R.E., Quickenden, T.I., 1997. Photolysis and radiolysis of water ice on outer solar system bodies. J. Geophys. Res. 102, 10,985–10,996.

Johnson, R.E., Lanzerotti, L.J., Brown, W.L., 1982. Planetary applications of condensed gas sputtering. Nucl. Instrum. Methods 198, 147.

Johnson, R.E., Killen, R.M., Waite, J.H., Lewis, W.S., 1998. Europa's surface and sputter-produced ionosphere. Geophys. Res. Lett. 25, 3257–3260.

Jordan, T.H., Streib, W.E., Smith, H.W., Liscombe, W.N., 1964. Single crystal studies of β-F_2 and γ-O_2. Acta Cryst. 17, 777–778.

Kjaergaard, H.G., Low, G.R., Robinson, T.W., Howard, D.L., 2002. Calculated OH-stretching vibrational transitions in the water-nitrogen and water-oxygen complexes. J. Phys. Chem. A 106, 8902–8955.

Krupenie, P.H., 1972. The spectrum of molecular oxygen. J. Phys. Chem. Ref. Data 1, 423–520.

Landau, A., Allin, E.J., Welsh, H.L., 1962. The absorption spectrum of solid oxygen in the wavelength region from 12,000 Å to 3300 Å. Spectrochim. Acta 18, 1–19.

Long, C.A., Ewing, G.E., 1971. The infrared spectrum of bound state oxygen dimers in the gas phase. Chem. Phys. Lett. 9, 225–229.

Matich, A.J., Bakker, M.G., Lennon, D., Quickenden, T.I., Freeman, C.G., 1993. O_2 luminescence from UV-excited H_2O and D_2O ices. J. Phys. Chem. 97, 10,539–10,553.

McCord, T.B., Carlson, R.W., Smythe, W.D., Hansen, G.B., Clark, R.N., Hibbitts, C.A., Fanale, F.P., Granahan, J.C., Segura, M., Matson, D.L.,

Johnson, T.V., Martin, P.D., 1997. Organics and other molecules in the surfaces of Callisto and Ganymede. Science 278, 271–275.

McCord, T.B., Hansen, G.B., Matson, D.L., Johnson, T.V., Crowley, J.K., Fanale, F.P., Carlson, R.W., Smythe, W.D., Martin, P.D., Hibbitts, C.A., Granahan, J.C., Ocampo, A., 1999a. Hydrated salt minerals on Europa's surfaces from the Galileo near-infrared mapping spectrometer (NIMS) investigation. J. Geophys. Res. 104, 11,827–11,851.

McCord, T.B., Hansen, G.B., Shirley, J.H., Carlson, R.W., 1999b. Discussion of the 1.04-µm water ice absorption band in Europa NIMS spectra and a new NIMS calibration. J. Geophys. Res. 104, 27,157–27,162.

McGrath, M.A., Feldman, P.D., Strobel, D.F., Retherford, K., Wolven, B., Moos, H.W., 2000. HST/STIS Ultraviolet Imaging of Europa. Bull. AAS. DPS 2000.

Mèrienne, M., Jenouvrier, A., Coquart, B., Carleer, M., Fally, S., Colin, R., Vandaele, A.C., Hermans, C., 2000. Fourier transform, spectroscopy of the O_2 Herzberg bands. II. Band oscillator strengths and transition moments. J. Mol. Spectrosc. 202, 171–193.

Molina, L.T., Schinke, S.D., Molina, M.J., 1977. Ultraviolet absorption spectrum of hydrogen peroxide vapor. Geophys. Res. Lett. 4, 580–582.

Moore, M.H., Hudson, R.L., 2000. IR detection of H_2O_2 at 80 K in ion-irradiated laboratory ices relevant to Europa. Icarus 145, 282–288.

Mulliken, R.S., 1928. Interpretation of the atmospheric bands of oxygen. Phys. Rev. 32, 880–887.

Newnham, D.A., Ballard, J., 1998. Visible absorption cross sections and integrated absorption intensities of molecular oxygen (O_2 and O_4). J. Geophys. Res. 103, 28,801–28,816.

Noll, K.S., Johnson, R.E., Lane, A.L., Domingue, D.L., Weaver, H.A., 1996. Detection of ozone on Ganymede. Science 273, 341–343.

Noll, K.S., Roush, T.L., Cruishank, D.P., Johnson, R.E., Pendleton, Y.J., 1997. Detection of ozone on Saturn's satellites Rhea and Dione. Nature 388, 45–47.

Orton, G.S., Spencer, J.R., Travis, L.D., Martin, T.Z., Tamppari, L.K., 1996. Galileo photopolarimeter-radiometer observations of Jupiter and the Galilean satellites. Science 274, 389–391.

Palmer, I.J., Byers Brown, W., Hillier, I.H., 1996. Simulation of the charge-transfer absorption of the H_2O/O_2 van der Waals complex using high level ab initio calculations. J. Chem. Phys. 104, 3198–3204.

Reimann, C.T., Boring, J.W., Johnson, R.E., Garrett, J.W., Farmer, K.R., Brown, K.J., Marcantonio, W.L., Augustyniak, W.M., 1984. Ion-induced molecular ejection from D_2O ice. Surf. Sci. 147, 227–240.

Roder, H.M., 1978. The molar volume (density) of solid oxygen in equilibrium with vapor. J. Phys. Chem. Ref. Data 7, 949–957.

Romand, M.J., Granier-Mayence, J., 1954. Spectre d'absorption de l'oxygène solide entre 2000 et 4500 Å. J. Phys. Radium 15, 62–63.

Shardanand, 1969. Absorption cross sections of O_2 and O_4 between 2000 and 2800 Å. Phys. Rev. 186, 5–9.

Sieger, M.T., Simpson, W.C., Orlando, T.M., 1998. Production of O_2 on icy satellites by electronic excitation of low-temperature water ice. Nature 394, 554–556.

Slanger, T.G., Cosby, P.C., 1988. O_2 spectroscopy below 5.1 eV. J. Phys. Chem. 92, 267–282.

Smith, K.M., Newnham, D.A., 1999. Near-infrared absorption spectroscopy of oxygen and nitrogen gas mixtures. Chem. Phys. Lett. 308, 1–6.

Smith, K.M., Newnham, D.A., 2000. Near-infrared absorption cross sections and integrated absorption intensities of molecular oxygen (O_2, O_2–O_2, and O_2–N_2). J. Geophys. Res. 105, 7383–7396.

Spencer, J.R., Calvin, W.M., 2002. Condensed O_2 on Europa and Callisto. Astron. J., submitted for publication.

Spencer, J.R., Calvin, W.M., Person, M.J., 1995. CCD spectra of the Galilean satellites: molecular oxygen on Ganymede. J. Geophys. Res. 100, 19,049–19,056.

Svishchev, I.M., Boyd, R.J., 1998. Van der Waals complexes of water and oxygen and nitrogen: infrared spectra and atmospheric implications. J. Phys. Chem. A 102, 7294–7296.

Taub, I.A., Eiben, K., 1968. Transient solvated electron, hydroxyl, and hydroperoxy radicals in pulse-irradiated crystalline ice. J. Chem. Phys. 49, 2499–2513.

Vaida, V., Headrick, J.E., 2000. Physicochemical properties of hydrated complexes in the earth's atmosphere. J. Phys. Chem. A 104, 5401–5412.

Vidal, R.A., Bahr, D.A., Baragiola, R.A., Peters, M., 1997. Oxygen on Ganymede: laboratory studies. Science 276, 1839–1842.

Westley, M., Baragiola, R.A., Johnson, R.E., Baratta, G., 1995. Photo desorption from low temperature water ice: astrophysical implications. Nature 373, 405–407.